The Use of Wastewater Surveillance to Estimate SARS-CoV-2 Fecal Viral Shedding Pattern and Identify Time Periods with Intensified Transmission

Wan Yang,[1*] Enoma Omoregie,[2] Aaron Olsen,[2] Elizabeth A. Watts,[2,3] Hilary Parton,[2] Ellen Lee[2]

[1]Department of Epidemiology, Columbia University, New York, NY, USA; [2]New York City Department of Health and Mental Hygiene, Queens, NY, USA; [3]Centers for Disease Control and Prevention, Atlanta, GA, USA

*Correspondence to: wy2202@cumc.columbia.edu

ABSTRACT

Background: Wastewater-based surveillance is an important tool for monitoring the COVID-19 pandemic. However, it remains challenging to translate wastewater SARS-CoV-2 viral load to infection number, due to unclear shedding patterns in wastewater and potential differences between variants.

Objectives: We utilized comprehensive wastewater surveillance data and estimates of infection prevalence (i.e., the source of the viral shedding) available for New York City (NYC) to characterize SARS-CoV-2 fecal shedding pattern over multiple COVID-19 waves.

Methods: We collected SARS-CoV-2 viral wastewater measurements in NYC during August 31, 2020 – August 29, 2023 (N = 3794 samples). Combining with estimates of infection prevalence (number of infectious individuals including those not detected as cases), we estimated the time-lag, duration, and per-infection fecal shedding rate for the ancestral/Iota, Delta, and Omicron variants, separately. We also developed a procedure to identify occasions with intensified transmission.

Results: Models suggested fecal viral shedding likely starts around the same time as and lasts slightly longer than respiratory tract shedding. Estimated fecal viral shedding rate was highest during the ancestral/Iota variant wave, at 1.44 (95% CI: 1.35 – 1.53) billion RNA copies in wastewater per day per infection (measured by RT-qPCR), and decreased by ~20% and 50-60% during the Delta wave and Omicron period, respectively. We identified around 200 occasions during which the wastewater SARS-CoV-2 viral load exceeded the expected level in any of 14 sewersheds. These anomalies disproportionally occurred during late January, late April - early May, early August, and from late-November to late-December, with frequencies exceeding the expectation assuming random occurrence ($P < 0.05$; bootstrapping test).

Discussion: These estimates may be useful in understanding changes in underlying infection rate and help quantify changes in COVID-19 transmission and severity over time. We have also demonstrated that wastewater surveillance data can support the identification of time periods with potentially intensified transmission.

INTRODUCTION

Since the early phase of the COVID-19 pandemic, studies have reported that wastewater SARS-CoV-2 viral loads often closely track or lead case and/or hospitalization trajectories and, as such, can serve as a cost-effective surveillance tool for monitoring the COVID-19 pandemic.[1-5] Thus, wastewater-based surveillance systems have been built worldwide on local and national scales. With decreasing clinical testing and genomic sequencing,[6,7] there has been increased interest in wastewater surveillance, given results are generated independently of clinical testing practice.

Though there are advantages of SARS-CoV-2 wastewater surveillance, a large US national survey of public health agencies completed in 2022 noted the results were often deemed supplementary to surveillance involving clinical laboratory tests.[8] One of the hurdles is that while the trends could indicate changes in SARS-CoV-2 community circulation, it remains challenging to directly translate wastewater SARS-CoV-2 viral loads to a specific number of infections in the population, due to the unclear fecal viral shedding rate (after accounting for the recovery rate of virus genomes) in wastewater samples. In addition, with the fast emergence and turnover of new SARS-CoV-2 variants, it is unclear how fecal shedding of the virus may have altered over time by variant. To address these questions, we utilize comprehensive wastewater surveillance data and estimates of infection prevalence (i.e., the source of the viral shedding) available for New York City (NYC) to characterize SARS-CoV-2 fecal shedding over multiple COVID-19 pandemic and epidemic waves.

NYC experienced the earliest pandemic wave in the United States (US), and shortly after the initial wave, established a wastewater surveillance program that covers all of its 14 sewersheds which serve over 8 million residents.[2] Since August 31, 2020, the program has continuously measured SARS-CoV-2 viral load weekly. Independently, we have developed and used a comprehensive model-inference system – calibrated to case, emergency department (ED) visit, and mortality data – to reconstruct the underlying transmission dynamics and estimate key epidemiological characteristics.[9,10] In particular, the model-inference system estimates the number of infectious individuals including those not detected as cases (i.e., infection prevalence) in each of the city's 42 neighborhoods during each week since March 1, 2020.[9,10] Combining the wastewater SARS-CoV-2 viral load data and infection prevalence estimates over a 3-year period (i.e., August 31, 2020 – August 29, 2023), we are able to characterize the viral shedding pattern (i.e., time-lag, duration, and *per-infection* shedding rate) for the ancestral/Iota, Delta, and Omicron variants, separately. We are also able to identify time periods with greater transmission.

METHODS

SARS-CoV-2 wastewater surveillance data.

The SARS-CoV-2 wastewater surveillance program in NYC started on August 31, 2020. Wastewater samples were taken at each of the city's 14 wastewater treatment plants, usually twice per week on Sundays and Tuesdays (*N* = 3794 samples; see variations and details in Table S1). SARS-CoV-2 RNA concentration was measured using quantitative reverse transcription polymerase chain reaction (RT-qPCR) assays during August 31, 2020, through April 11, 2023, and reverse transcription digital PCR (RT-dPCR) assays from November 1, 2022, through August 29, 2023. All measurements adjusted for sewershed-specific flow rate and service population size. Specifically, per-capita SARS-CoV-2 viral load (RNA copies per day per population) was computed as the viral concentration measure multiplied by the daily sewage flow rate and then divided by the service population.

For weeks after April 11, 2023, when the samples were measured using RT-dPCR alone, we converted the RT-dPCR measurements to RT-qPCR equivalents, to allow characterization of SARS-CoV-2 viral shedding during the entire Omicron period. Specifically, we first computed the conversion ratio using measurements from November 1, 2022, through April 11, 2023, when both assays were conducted, simply as the mean of all RT-qPCR measurements dividing the mean of all RT-dPCR measurements, during these weeks. We then multiplied the RT-dPCR measurements by the conversion ratio to obtain the converted RT-qPCR equivalents. As an alternative, we stratified the data by sewershed and performed the conversion using sewershed-specific conversion ratios (see Sensitivity Analysis). In addition, the RT-qPCR and RT-dPCR measures differed substantially (by a factor of 16.7 based on the aforementioned overlapping measurements), likely due to difference in methodology.[11] To facilitate comparison with studies primarily using RT-dPCR, we also converted all RT-qPCR measurements to RT-dPCR equivalents when reporting the viral shedding rates.

SARS-CoV-2 infection prevalence estimates.

Estimated SARS-CoV-2 infection prevalence came from a model-inference system,[12] independent of the wastewater surveillance data. Briefly, the model-inference system fit a neighborhood-level Susceptible-Exposed-Infectious-(re)Susceptible-Vaccination (SEIRSV) model to age-grouped, neighborhood-specific COVID-19 case, ED visit, and mortality data, accounting for concurrent nonpharmaceutical interventions, vaccinations, under-detection of infection, and seasonal changes. We used the SEIRSV model to explicitly simulate the number of infectious individuals – i.e., anyone who can actively transmit SARS-CoV-2 and infect others regardless of symptoms and test-seeking behaviors – present in the population and estimated this infection prevalence during each week using the full model-inference system using COVID-19 case, ED visit, and mortality data.[12] That is, similar to the wastewater SARS-CoV-2 viral loads

measuring the total population fecal shedding regardless of clinical testing, estimated infection prevalence here included all individuals actively transmitting SARS-CoV-2 (primarily via shedding from the respiratory tracts) regardless of whether they were detected as cases.

The infection prevalence estimates are United Hospital Fund neighborhood-[13] and age group specific, and available for each week starting March 1, 2020 (the pandemic onset in NYC) to the week starting August 27, 2023. To match with the sewershed-level wastewater SARS-CoV-2 viral load data, we first mapped each neighborhood (42 in total vs. 14 sewersheds) to the corresponding sewershed based on geolocation; if a neighborhood overlapped multiple sewersheds, we assigned it to the one with the maximal overlap. For each sewershed and week, we then aggregated all estimated infectious individuals from all related neighborhoods.

Estimating the fecal viral shedding time-lag, duration, and rate.

To analyze the fecal viral shedding pattern by variant, we defined three time periods based on data availability and the predominant circulating variant[14] (i.e., to be more variant-specific): i) the 2nd wave (predominantly the ancestral and Iota variants), from August 31, 2020 (i.e., the first day of wastewater surveillance) through June 26, 2021; ii) the Delta wave (predominantly the Delta variant), from June 27, 2021 (i.e., the first week the share of Delta exceeding 50% among the sequenced specimens) through December 4, 2021; and iii) the Omicron period (predominantly Omicron subvariants and included multiple Omicron-subvariant waves), from December 5, 2021 (i.e., the first week the share of Omicron BA.1 exceeding 25% among the sequenced samples; note that we used a lower threshold here given the milder severity of Omicron BA.1[15] and thus likely fewer infections detected and sequenced) though August 29, 2023 (i.e., the last wastewater sample during the study period).

SARS-CoV-2 viral load in wastewater represents the pooled fecal shedding of the virus by the population, whereas the infection prevalence represents the proportion of population actively infectious at a given time (i.e., the source of the viral shedding after a potential time-lag). Thus, to estimate the viral shedding rate for each variant (per the time period defined above), we used a linear regression model, accounting for circulating variants and spatial variations by sewershed, per Eq. 1:

$$VL_{t\in\{t\}+\tau} = \beta_0 + \beta_1 Sewershed + \beta_2 I_t + \beta_3 Period_t + \beta_4 I_t Period_t \quad \text{(Eq. 1)}$$

where, $VL_{t\in\{t\}+\tau}$ is the wastewater SARS-CoV-2 viral load measured during time-window $\{t\}$, adjusted by a time-lag or lead of τ days (see details below); *Sewershed* is a categorical variable (*Sewershed* = one of the 14 sewersheds in the city) to account for spatial variation; I_t is the infection prevalence estimated for week-t; and $Period_t$ represents three epidemic time

periods as defined above, included as a proxy for circulating variants during week-*t* (*Period* = 2nd wave, Delta wave, or Omicron period, as defined above). The interaction term $I_t Period_t$ is included to account for potential nonadditive interaction of the two variables (here, in essence, to allow different viral shedding rates by variant). Per Eq. 1, we computed the estimates of fecal viral shedding rate for each variant using the coefficients β_2 and β_4.

Given the different surveillance schedules and likely difference between fecal and respiratory viral shedding, we tested three sliding time-windows (i.e., $\{t\}$ in Eq. 1) for matching the wastewater measurements (twice per week, representing fecal shedding) with the infection prevalence estimates (weekly estimates, representing respiratory shedding); specifically, we averaged 2, 3, or 4 consecutive wastewater samples, corresponding to roughly a 1-, 1.5-, or 2-week window, respectively, depending on the wastewater sampling schedule and time-adjustment used. For each time-window $\{t\}$, to identify a proper time-adjustment (τ in Eq. 1), we tested five settings to capture the time difference from becoming infectious via respiratory shedding to fecal shedding per the population-level surveillance data:

i) a 6- to 7-day lead, i.e., the wastewater samples included in time-window $\{t\}$ started from the 1st sample taken *the week before* the infection prevalence estimate; note the 1st sample was taken on Sunday (corresponding to a maximum of 7-day lead) or Monday (corresponding to a maximum of 6-day lead);
ii) a 4- to 5-day lead, i.e., the wastewater samples included in time-window $\{t\}$ started from the 2nd sample taken *the week before* the infection prevalence estimate; note the 2nd sample was taken on Tuesday (corresponding to a maximum of 5-day lead) or Wednesday (corresponding to a maximum of 4-day lead);
iii) concurrent (no time-difference, τ=0), i.e., the wastewater samples included in time-window $\{t\}$ started from the 1st sample taken *the week of* the infection prevalence estimate;
iv) a 2- to 3-day lag, i.e., the wastewater samples included in time-window $\{t\}$ started from the 2nd sample taken *the week of* the infection prevalence estimate (a Tuesday sample corresponded to a 2-day lag and a Wednesday sample corresponded to a 3-day lag); and
v) a 7- to 8-day lag, i.e., the wastewater samples included in time-window $\{t\}$ started from the 1st sample taken *the week after* the infection prevalence estimate (a Sunday sample corresponded to a 7-day lag and a Monday sample corresponded to a 8-day lag).

In addition, we performed variant/period-specific analyses for each of the three time-periods defined above, using a similar model form as Eq. 1 but without the terms related to time-period ($Period_t$). Since the Omicron period included multiple Omicron-subvariant waves, we also performed stratified analyses for the Omicron BA.1 wave (December 5, 2021, through March 4,

2022, i.e., the last week the share of Omicron BA.1 exceeding 50%) and for weeks from March 5, 2022 onwards, separately.

Identifying timings with higher-than-expected transmission

Visual inspection of the wastewater data showed there were occasional spikes in SARS-CoV-2 viral load, potentially due to intensified transmission. Due to the temporal dynamics and sampling noise, it is challenging to distinguish such potential instances (i.e., a true signal) based on the wastewater data alone. Thus, here we used the infection prevalence estimates, which had accounted for the main underlying transmission factors, to construct the expected SARS-CoV-2 viral load for comparison. Specifically, we first computed the daily infection prevalence using the weekly estimates with a spline smoothing function, and then used those as inputs in Eq. 1 to compute the expected daily SARS-CoV-2 viral load (median and 90% confidence intervals [CI]). Given the large variance in both the infection prevalence estimates and SARS-CoV-2 viral load data, we deemed a wastewater measurement higher than expected, if it was higher than the 95th percentile (i.e., the upper bound of the 90% CI) of the expected SARS-CoV-2 viral load.

To examine the timing with higher-than-expected SARS-CoV-2 viral load, we grouped the identified anomaly dates into 10-day bins based on calendar time, i.e., the 1st (early), 2nd (mid), and last (late) 10 days of each month; for example, January 1 of 2021, January 5 of 2022, and January 10 of 2023 would all be grouped as "early-January". This allows recurrent and/or seasonal events to be grouped in the same or nearby bins. To test whether the identified anomalies occurred at random (e.g., due to noise in the data), we further performed a bootstrap test with 5000 random samples. For each bootstrapping set, we randomly sampled $n_{anomaly}$ (i.e., the number of identified anomalies) dates from the wastewater measurements (N = 3794), and then grouped the dates into the same 10-day bins as done for the identified anomalies. We then pooled the 5000 sets together to construct the distribution of each timing. For example, for early-January (the first 10-day calendar bin), with n_1, n_2, …, and n_{5000} of the dates falling in that bin for the 5000 sets, the likelihood of having k (k= 0, …, $n_{anomaly}$, i.e., from none to all) anomalies during early-January would be:

$$P(x = k) = \frac{number\ of\ n_i{=}k\ among\ the\ 5000\ bootsrapping\ samples}{5000};$$

and the likelihood of having k or more anomalies during early-January would be:

$$P(x \geq k) = \frac{number\ of\ n_i{\geq}k\ among\ the\ 5000\ bootsrapping\ samples}{5000}.$$

Sensitivity Analyses

In a first sensitivity analysis, we only included SARS-CoV-2 viral load measured by RT-qPCR (i.e., August 31, 2020– April 11, 2023), to examine if the viral shedding rate estimates were affected

by converting RT-dPCR measurements to RT-qPCR equivalents due to changes in testing assays. In a second sensitivity analysis, we included all SARS-CoV-2 viral load measurements but used the sewershed-specific conversion ratios instead of the citywide conversion ratio for all sewersheds.

RESULTS

General trends in measured wastewater SARS-CoV-2 viral load and estimated infection prevalence.

During the 3-year study period (August 31, 2020 – August 29, 2023), trends in wastewater SARS-CoV-2 viral load were generally consistent with the trends in estimated infection prevalence (Fig 1). Across the 14 NYC sewersheds (Fig 1A), wastewater SARS-CoV-2 viral load tended to rise and fall around the same time (Fig 1B-D and Figs S1-3), indicating epidemic waves were highly synchronized across the city. However, the magnitudes of wastewater SARS-CoV-2 viral load and infection prevalence estimates both varied substantially over time and across sewersheds and may not scale consistently. For example, even though certain sewersheds tended to detect higher SARS-CoV-2 viral loads than others, the rankings changed across different waves (see Fig S1-3, ranked by average viral load). Similar spatial heterogeneity was apparent in the estimated infection prevalence and the discrepancies between wastewater SARS-CoV-2 viral load and estimated infection prevalence appeared larger during the 2nd wave (Fig S1). Such spatial heterogeneity is not unexpected, since several factors such as RNA degradation[16] and dilution,[16] and the contribution of infected animals[17] could all vary by sewershed, and ultimately affect wastewater measurements. In addition, uncertainty in the infection prevalence estimate could also vary by sewershed (e.g., larger uncertainty for those with smaller population size; see, e.g., the wider uncertainty bounds for Oakwood Beach sewershed in Fig S1).

Estimated fecal viral shedding patterns.

Using the wastewater SARS-CoV-2 viral load data and infection prevalence estimates (i.e., source of fecal viral shedding), we examined fecal viral shedding patterns over the entire study period or stratified by variant/time-period, separately. The estimates are generally consistent (Table 1). Among the 15 combinations of fecal viral shedding time-differences and durations tested, the main model (including all waves) identified concurrent infection prevalence estimates (i.e., no time-difference between becoming infectious via respiratory shedding and fecal shedding) and SARS-CoV-2 viral load aggregated over 3 wastewater samples (2 during the same week and 1 in the beginning of the following week, i.e., a 8- to 9- day-time-interval) as the best setting (highest adjusted R-squared; Fig 2A). Using a 4-5-day-lead and aggregation over 4 wastewater samples (i.e., one sample 4-5 days before, two during, and one 1-2 days after the infection prevalence estimate) led to the second-best model fit (Fig 2A, 2nd dark bar), and was

the best setting for the Delta wave and weeks after the BA.1 wave in the stratified analysis (Table 1). Model fit degraded quickly with changing time-differences (both leads and lags), when only 2 (roughly a 1-week duration) or 3 (roughly a 1.5-week duration) wastewater samples were included.

Estimated fecal viral shedding rate was highest for infections during the 2nd wave (mostly due to the ancestral and Iota variants), at 1.44 (95% CI: 1.35 – 1.53) billion RNA copies by RT-qPCR in wastewater per day per infectious person [or 24 (95% CI: 22.49 - 25.51) billion RNA copies per RT-dPCR conversion; see Methods]. The estimated rate decreased by ~20% during the subsequent Delta wave and by 50-60% during the Omicron period (Table 1). Importantly, we note the lower estimates for Delta and Omicron may in part reflect reduced shedding among vaccinees and recoverees, in addition to variant-specific variations.

Timings with higher-than-expected transmission

The infection prevalence estimates have accounted for the general transmission factors (here, population-level mobility, vaccinations, variant-specific properties, and seasonal risk of infection; see Methods), but may have not fully accounted for activities such as increased gatherings during certain time-periods that might increase transmission. In contrast, wastewater SARS-CoV-2 viral load is a composite measure of all transmission events. Thus, comparison of these two quantities could support identification of such events. Following a procedure designed per this mechanism (see Methods), we identified 198 occasions where wastewater SARS-CoV-2 viral loads exceeded the expected levels in any of the 14 sewersheds (see Fig 3A for identified anomalies for Newtown Creek, the sewershed with the largest service population). These anomalies disproportionally occurred during late January, late April - early May, early August, and mid-November to late-December (Fig 3B), with frequencies exceeding the expectation assuming random occurrence. Among the 5000 bootstrapping sets, none had as many or more anomalies as observed in early August or late November ($P = 0$) and less than 5% had as many or more anomalies as observed in late January, late April, early May, late November, and late December ($P < 0.05$ for all these calendar bins; Table S2).

Sensitivity analyses

Results from the two sensitivity analyses are consistent with the main analysis. In the 1st sensitivity analysis (i.e., using SARS-CoV-2 viral load measured by RT-qPCR alone, for a shorter study period from 8/31/20 to 4/11/23), similar fecal viral shedding rates were estimated (Table S3). The 2nd sensitivity analysis (using sewershed-specific conversion ratios to convert the RT-dPCR measurements after 4/11/23, same study period as the main analysis) estimated the same fecal viral shedding rates as the main analysis, and identified three additional anomalies (i.e., 1 in late-January, 1 in mid-August, and 1 in early-July).

DISCUSSION

Wastewater surveillance can be a valuable tool for monitoring SARS-CoV-2 circulation in the population. To further develop understanding of wastewater surveillance data, we have combined independent model-inference estimates of infection prevalence to characterize fecal viral shedding patterns for multiple major SARS-CoV-2 variants. Using NYC as an example, we have also demonstrated that these data and estimates can support the identification of time periods with potentially intensified transmission.

Importantly, here we examined how wastewater SARS-CoV-2 viral shedding is related to estimated infection prevalence, rather than health outcomes as in previous studies. This choice could lead to certain apparent differences but has several advantages. First, previous studies have reported detection of SARS-CoV-2 in wastewater (e.g., an increase in viral load, or the presence of a new variant) several days ahead of the detection of cases, hospitalizations, or deaths, due to the delay in health outcomes.[18-20] Here, infection prevalence is a proxy of respiratory tract shedding, which could precede fecal viral shedding. Indeed, we found wastewater SARS-CoV-2 viral loads measured round 1.5 week of the infection prevalence estimate afforded the best model fit (Table 1). This finding suggests that fecal viral shedding likely starts around the same time an individual becomes infectious and lasts slightly longer than the shedding from respiratory tract. Consistent with our finding, studies have shown that fecal SARS-CoV-2 RNA was detectable in patients within the first week of COVID-19 diagnosis and could last longer than respiratory shedding.[16,21]

Second, case-, hospitalization-, or death-to-wastewater-viral-load ratio could decrease with increased vaccinations/reinfections and circulation of milder variants (e.g., Omicron) due to reduced severity or testing, and such reductions have been reported.[19,22] In contrast, as our estimates included all infections regardless of severity or testing, the infection-to-wastewater-viral-load ratio (roughly, the inverse of estimated per-infection fecal viral shedding rate; Table 1) is relatively stable during each variant wave. For example, the wave-stratified analysis estimated similar fecal viral shedding rates for the BA.1 wave and weeks after BA.1 (Table 1). Importantly, using the infection prevalence estimates, we are able to quantify the fecal viral shedding rate for each major SARS-CoV-2 variant/time-period (Table 1). These estimates can be used to account for changes in underlying infection rate during this study period (e.g. converting wastewater SARS-CoV-2 viral loads to infection prevalence per Table 1) and help examine changes in COVID-19 severity (e.g., changes in hospitalization rate and infection-fatality risk). Such wastewater-viral-load and infection-based estimates may be more accurate than case-based measures, which are subject to test-seeking biases.

Third, previous studies have measured viral loads in clinical samples from the respiratory tract. Based on the reported cycle threshold (CT) values, the respiratory tract viral load was higher in Delta and Omicron infections than the ancestral variant,[23-28] consistent with the higher infectiousness of these variants of concern. In contrast, fecal viral shedding is not a main mode of transmission,[29,30] and here using variant circulation time-period as a proxy, we estimate that the fecal viral shedding rate was the highest for the ancestral/Iota variants, followed by Delta (~20% lower), and then Omicron (~50-60% lower; Table 1). Early studies of ancestral SARS-CoV-2 infections found that patients with diarrhea shed more viruses than patients without diarrhea (see, e.g., a review in ref. [16]), suggesting fecal viral shedding may be associated with diarrhea. In addition, studies found that vaccinations reduced the number of diarrhea episodes,[31] and that rates of diarrhea were highest among patients infected with the ancestral SARS-CoV-2, followed by patients infected with Delta and then Omicron.[32,33] Our estimates are consistent with the fecal viral shedding studies,[16,31-33] and support a difference in viral load between SARS-CoV-2 fecal shedding and respiratory tract shedding, in addition to the timing difference noted above.

In addition to characterizing SARS-CoV-2 fecal viral shedding pattern, we are also able to identify certain time-periods with intensified transmission. In NYC, analysis based on calendar timing showed likely intensified transmission during late-November through December (Fig 3B). Increased transmission also occurred during early August and late January. It is possible that other factors such as travel, holidays, or specific COVID-19 sub-variants could help explain these periods of intensified transmission, but further investigation is needed to determine their impact.

Lastly, we note several limitations. First, given the biweekly sampling dates for wastewater and weekly estimates for infection prevalence, we were unable to test finer time-differences and durations when examining SARS-CoV-2 fecal shedding pattern. Second, the estimates here were based on population data and thus represent an average of all individuals undergoing different disease stages in the population. As such, the estimated fecal shedding duration may be shorter than that reported in studies based on individual patient data (e.g., days or weeks after respiratory tract samples became negative[16]). Third, our infection prevalence estimates have accounted for the main transmission factors, through the information encapsulated in the COVID-19 case, ED visit, and mortality data used for model estimation. Thus, the expected SARS-CoV-2 viral load constructed using these estimates and in turn the identified anomalies are both conservative estimates and may have missed additional anomalies. In addition, wastewater collected from sewersheds may represent individuals who are residents of NYC as well as outside NYC, while infection prevalence estimates are based on NYC residents only.

In summary, we have characterized the fecal viral shedding pattern of SARS-CoV-2 in wastewater in New York City from 2020-2023. These estimates can be used to account for changes in underlying infection rate and help more accurately quantify changes in COVID-19 transmission and severity over time. We have also demonstrated that wastewater surveillance data combined with model-inference estimates can support the identification of time-periods that potentially intensify transmission. Additional studies are needed to better understand these periods and the potential to mitigate SARS-Cov-2 transmission.

Acknowledgements:
This study was supported by the National Institute of Allergy and Infectious Diseases (AI175747) and Centers for Disease Control and Prevention (CDC) and the Council of State and Territorial Epidemiologists (CSTE; contract no.: NU38OT00297). The authors thank Lauren Firestein for overseeing the data use agreement and facilitating data sharing for this project; Ramona Lall for providing syndromic surveillance emergency department data; Wenhui Li for providing COVID-19-associated mortality data; Iris Cheng for providing immunization data; Jubayer Ahmed, Nelson De La Cruz, and Brandon Nguyen for managing and providing wastewater data; the NYC DOHMH Respiratory Pathogens data team for overarching data management and provision of data for this project; and Shama Ahuja, Sharon Greene, Scott Harper, Elizabeth Luoma, Ulrike Siemetzki-Kapoor, Celia Quinn, and Faten Taki for their input on this manuscript.

Author contributions: WY designed the study, performed the analysis, and wrote the first draft; EO, AO, and EAW oversaw provision of the SARS-CoV-2 wastewater surveillance data; HP and EL oversaw provision of the COVID-19 case and emergency department visit data. All authors contributed to the final draft.

Conflict of interest:
The authors declare that they have no conflict of interest.

References:

1. Reynolds LJ, Gonzalez G, Sala-Comorera L, et al. SARS-CoV-2 variant trends in Ireland: Wastewater-based epidemiology and clinical surveillance. *Sci Total Environ*. Sep 10 2022;838(Pt 2):155828. doi:10.1016/j.scitotenv.2022.155828
2. Hoar C, Chauvin F, Clare A, et al. Monitoring SARS-CoV-2 in wastewater during New York City's second wave of COVID-19: sewershed-level trends and relationships to publicly available clinical testing data. *Environ Sci-Wat Res*. Mar 16 2022;doi:10.1039/d1ew00747e
3. Melvin RG, Chaudhry N, Georgewill O, Freese R, Simmons GE. Predictive power of SARS-CoV-2 wastewater surveillance for diverse populations across a large geographical range. *medRxiv*. Jan 30 2021;doi:10.1101/2021.01.23.21250376

4. Sanjuán R, Domingo-Calap P. Reliability of Wastewater Analysis for Monitoring COVID-19 Incidence Revealed by a Long-Term Follow-Up Study. Original Research. *Frontiers in Virology*. 2021-November-19 2021;1doi:10.3389/fviro.2021.776998
5. Schmitz BW, Innes GK, Prasek SM, et al. Enumerating asymptomatic COVID-19 cases and estimating SARS-CoV-2 fecal shedding rates via wastewater-based epidemiology. *Sci Total Environ*. Dec 20 2021;801:149794. doi:10.1016/j.scitotenv.2021.149794
6. Ungar L. Pandemic gets tougher to track as COVID testing plunges. Updated 5/10/2022. Accessed 8/16/2023, https://apnews.com/article/covid-us-testing-decline-14bf5b0901260b063e4fa444633f4d31
7. Arielle Mitropoulos, Brownstein J. Decline of testing, sequencing could hinder search for future COVID-19 variants, experts warn. 1/9/2024, Updated 3/30/2022. Accessed 1/9/2024, 2024. https://abcnews.go.com/Health/decline-testing-sequencing-hinder-search-future-covid-19/story?id=83727646
8. Keshaviah A, R.N. , Karmali DV, T. Huffman, X.C. Hu, Diamond MB. *The Role of Wastewater Data in Pandemic Management*. 2022.
9. Yang W, Kandula S, Huynh M, et al. Estimating the infection-fatality risk of SARS-CoV-2 in New York City during the spring 2020 pandemic wave: a model-based analysis. *The Lancet Infectious Diseases*. 2021;21(2):203-212. doi:10.1016/S1473-3099(20)30769-6
10. Yang W, Greene SK, Peterson ER, et al. Epidemiological characteristics of the B.1.526 SARS-CoV-2 variant. *Science Advances*. 2022;8(4):eabm0300. doi:doi:10.1126/sciadv.abm0300
11. Ahmed W, Smith WJM, Metcalfe S, et al. Comparison of RT-qPCR and RT-dPCR Platforms for the Trace Detection of SARS-CoV-2 RNA in Wastewater. *ACS ES&T Water*. 2022/11/11 2022;2(11):1871-1880. doi:10.1021/acsestwater.1c00387
12. Yang W, Parton H, Li W, Watts EA, Lee E, Yuan H. SARS-CoV-2 dynamics in New York City during March 2020 - August 2023. *medRxiv*. 2024:2024.07.19.24310728. doi:10.1101/2024.07.19.24310728
13. NewYork City Department of Health and Mental Hygiene. NYC UHF 42 Neighborhoods. http://a816-dohbesp.nyc.gov/IndicatorPublic/EPHTPDF/uhf42.pdf
14. New York City Department of Health and Mental Hygiene. Variants. https://github.com/nychealth/coronavirus-data/tree/master/variants
15. Wolter N, Jassat W, Walaza S, et al. Early assessment of the clinical severity of the SARS-CoV-2 omicron variant in South Africa: a data linkage study. *The Lancet*. 2022;399(10323):437-446. doi:10.1016/S0140-6736(22)00017-4
16. Foladori P, Cutrupi F, Segata N, et al. SARS-CoV-2 from faeces to wastewater treatment: What do we know? A review. *Sci Total Environ*. Nov 15 2020;743:140444. doi:10.1016/j.scitotenv.2020.140444
17. Meekins DA, Gaudreault NN, Richt JA. Natural and Experimental SARS-CoV-2 Infection in Domestic and Wild Animals. *Viruses*. Oct 4 2021;13(10)doi:10.3390/v13101993
18. Karthikeyan S, Levy JI, De Hoff P, et al. Wastewater sequencing reveals early cryptic SARS-CoV-2 variant transmission. *Nature*. Sep 2022;609(7925):101-108. doi:10.1038/s41586-022-05049-6
19. Hegazy N, Cowan A, D'Aoust PM, et al. Understanding the dynamic relation between wastewater SARS-CoV-2 signal and clinical metrics throughout the pandemic. *Science of the Total Environment*. Dec 20 2022;853doi:10.1016/j.scitotenv.2022.158458

20. Hopkins L, Persse D, Caton K, et al. Citywide wastewater SARS-CoV-2 levels strongly correlated with multiple disease surveillance indicators and outcomes over three COVID-19 waves. *Sci Total Environ*. Jan 10 2023;855:158967. doi:10.1016/j.scitotenv.2022.158967
21. Natarajan A, Zlitni S, Brooks EF, et al. Gastrointestinal symptoms and fecal shedding of SARS-CoV-2 RNA suggest prolonged gastrointestinal infection. *Med*. 2022;3(6):371-387. e9.
22. Nourbakhsh S, Fazil A, Li M, et al. A wastewater-based epidemic model for SARS-CoV-2 with application to three Canadian cities. *Epidemics-Neth*. Jun 2022;39doi:10.1016/j.epidem.2022.100560
23. Teyssou E, Delagreverie H, Visseaux B, et al. The Delta SARS-CoV-2 variant has a higher viral load than the Beta and the historical variants in nasopharyngeal samples from newly diagnosed COVID-19 patients. *J Infection*. Oct 2021;83(4):E1-E3. doi:10.1016/j.jinf.2021.08.027
24. Li B, Deng A, Li K, et al. Viral infection and transmission in a large, well-traced outbreak caused by the SARS-CoV-2 Delta variant. *medRxiv*. 2021:2021.07.07.21260122. doi:10.1101/2021.07.07.21260122
25. Yang Y, Guo L, Yuan J, et al. Viral and antibody dynamics of acute infection with SARS-CoV-2 omicron variant (B.1.1.529): a prospective cohort study from Shenzhen, China. *Lancet Microbe*. Aug 2023;4(8):e632-e641. doi:10.1016/S2666-5247(23)00139-8
26. Woodbridge Y, Amit S, Huppert A, Kopelman NM. Viral load dynamics of SARS-CoV-2 Delta and Omicron variants following multiple vaccine doses and previous infection. *Nat Commun*. Nov 7 2022;13(1):6706. doi:10.1038/s41467-022-33096-0
27. Migueres M, Dimeglio C, Mansuy JM, et al. Influence of Nasopharyngeal Viral Load on the Spread of the Omicron BA.2 Variant. *Clin Infect Dis*. Feb 8 2023;76(3):e514-e517. doi:10.1093/cid/ciac563
28. Imai K, Ikeno R, Tanaka H, Takada N. SARS-CoV-2 Omicron Variant in Human Saliva Samples in Cell-Free Form. *JAMA Netw Open*. Jan 3 2023;6(1):e2250207. doi:10.1001/jamanetworkopen.2022.50207
29. Wolfel R, Corman VM, Guggemos W, et al. Virological assessment of hospitalized patients with COVID-2019. *Nature*. May 2020;581(7809):465-469. doi:10.1038/s41586-020-2196-x
30. Albert S, Ruiz A, Peman J, Salavert M, Domingo-Calap P. Lack of evidence for infectious SARS-CoV-2 in feces and sewage. *Eur J Clin Microbiol Infect Dis*. Dec 2021;40(12):2665-2667. doi:10.1007/s10096-021-04304-4
31. Boulware DR, Murray TA, Proper JL, et al. Impact of Severe Acute Respiratory Syndrome Coronavirus 2 (SARS-CoV-2) Vaccination and Booster on Coronavirus Disease 2019 (COVID-19) Symptom Severity Over Time in the COVID-OUT Trial. *Clinical Infectious Diseases*. 2022;76(3):e1-e9. doi:10.1093/cid/ciac772
32. Pena Rodriguez M, Hernandez Bello J, Vega Magana N, et al. Prevalence of symptoms, comorbidities, and reinfections in individuals infected with Wild-Type SARS-CoV-2, Delta, or Omicron variants: a comparative study in western Mexico. *Front Public Health*. 2023;11:1149795. doi:10.3389/fpubh.2023.1149795
33. Torabi SH, Riahi SM, Ebrahimzadeh A, Salmani F. Changes in symptoms and characteristics of COVID-19 patients across different variants: two years study using neural network analysis. *BMC Infect Dis*. Nov 28 2023;23(1):838. doi:10.1186/s12879-023-08813-9

Table 1. Estimated patterns of SARS-CoV-2 fecal viral shedding in wastewater. Note in this study, SARS-CoV-2 RNA concentration was measured using quantitative reverse transcription polymerase chain reaction (RT-qPCR) assays during August 31, 2020, through April 11, 2023, and reverse transcription digital PCR (RT-dPCR) assays from November 1, 2022, through August 29, 2023. Based on samples tested using both assays, the RT-qPCR and RT-dPCR measures differed by a factor of 16.7. We used this conversion factor to convert measures from the two methods and provide estimates for RT-qPCR and RT-dPCR assays, separately.

model	wave	shedding rate (billion copies per day per infectious person, mean and 95% Confidence interval)	lag (days)	number of samples	adjusted R^2
Include all variant waves	2nd wave (08/31/20-06/26/21)	1.44 (1.35, 1.53) per qPCR; 24.0 (22.49, 25.51) per dPCR[a]	0	3	0.84
	Delta wave (06/27/21-12/04/21)	1.13 (0.86, 1.4) per qPCR; 18.9 (14.45, 23.35) per dPCR[a]	0	3	0.84
	Omicron period (12/05/21-08/29/23)	0.6 (0.59, 0.61) per qPCR; 9.96 (9.76, 10.16) per dPCR[b]	0	3	0.84
Stratified by wave/ period	2nd wave (08/31/20-06/26/21)	1.44 (1.37, 1.52) per qPCR; 24.07 (22.85, 25.28) per dPCR[a]	0	4	0.74
	Delta wave (06/27/21-12/04/21)	1.09 (0.91, 1.27) per qPCR; 18.14 (15.21, 21.08) per dPCR[a]	-5	4	0.37
	Omicron period (12/05/21-08/29/23)	0.6 (0.59, 0.61) per qPCR; 9.98 (9.76, 10.2) per dPCR[b]	0	3	0.86
	Omicron BA.1 (12/05/21-03/05/22)	0.59 (0.56, 0.61) per qPCR 9.78 (9.32, 10.23) per dPCR[a]	0	3	0.91
	After BA.1 (03/06/22-08/29/23)	0.72 (0.7, 0.75) per qPCR; 12.11 (11.72, 12.5) per dPCR[b]	-5	4	0.78

[a]RT-qPCR assays were used to measure SARS-CoV-2 RNA concentration during this period; the dPCR estimates were made by conversion (see Methods);

[b]RT-qPCR assays were used to measure SARS-CoV-2 RNA concentration through April 11, 2023 and RT-dPCR assays were used afterwards; conversion was used to obtain estimates for the entire period (see Methods).

Figures

Fig 1. Trends in wastewater SARS-CoV-2 viral load in the 14 sewersheds in NYC. The map in (A) shows 14 sewersheds (delineated by color) and 42 United Hospital Fund neighborhoods (delineated by lines). Dots show the per-capita SARS-CoV-2 viral load in each of the 14 sewersheds (right y-axis, in million copies per day per population by RT-qPCR; color coded per the legend) during the 2nd wave (B), Delta wave (C), and Omicron period (D). For comparison, we overlay the citywide estimates of infection prevalence (left y-axis; blue line = median; darker blue area = 50% CI and lighter blue area = 95% CI).

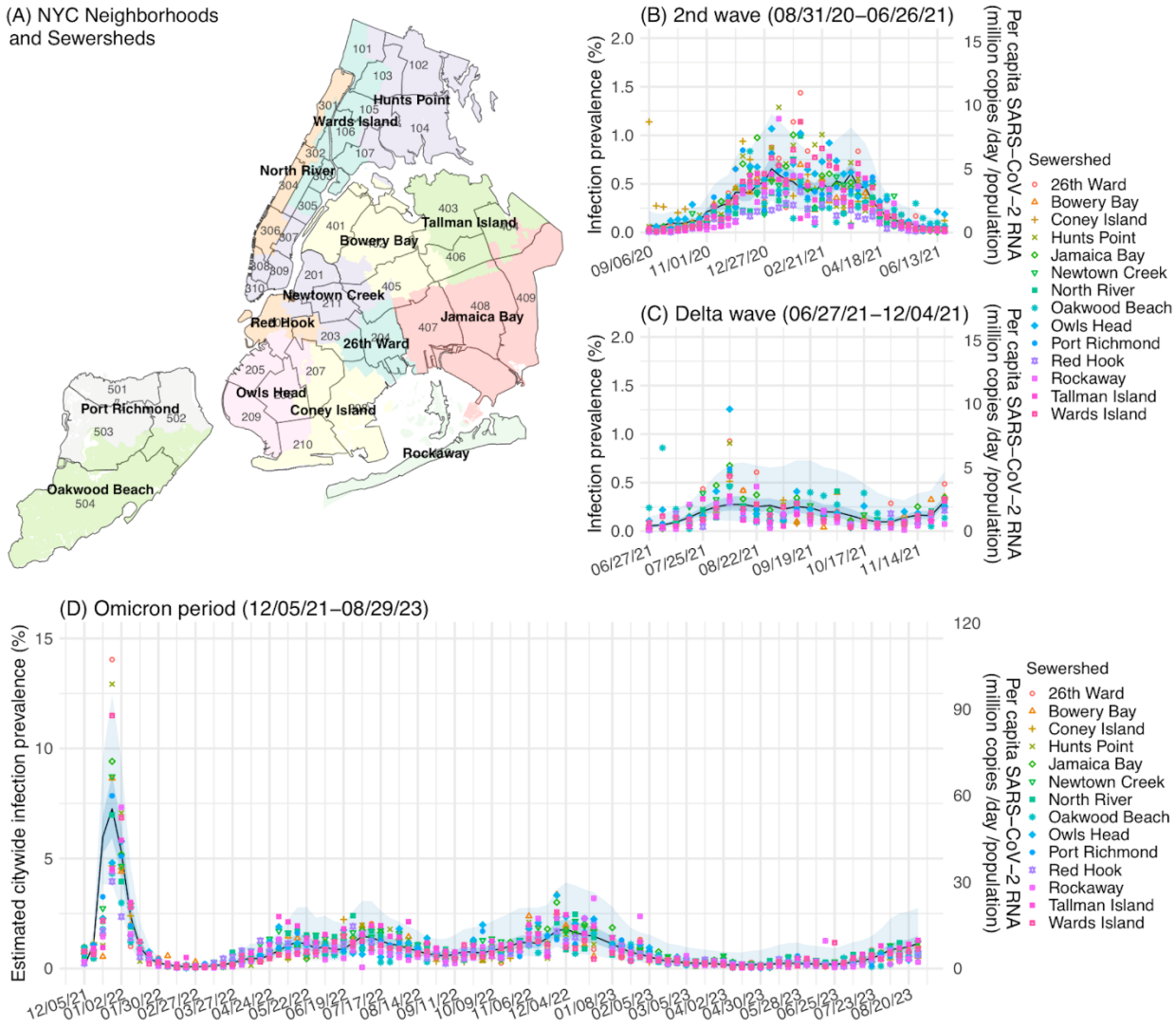

Fig 2. Model fit. (A) shows model performance based on the adjusted R-squared (higher number represents better performance) for different settings of time from becoming infectious to fecal viral shedding and time window of the wastewater samples are aggregated. The asterisk indicates the setting with the highest adjusted R-squared (i.e., best-fit model). (B) shows the model fit compared to the data.

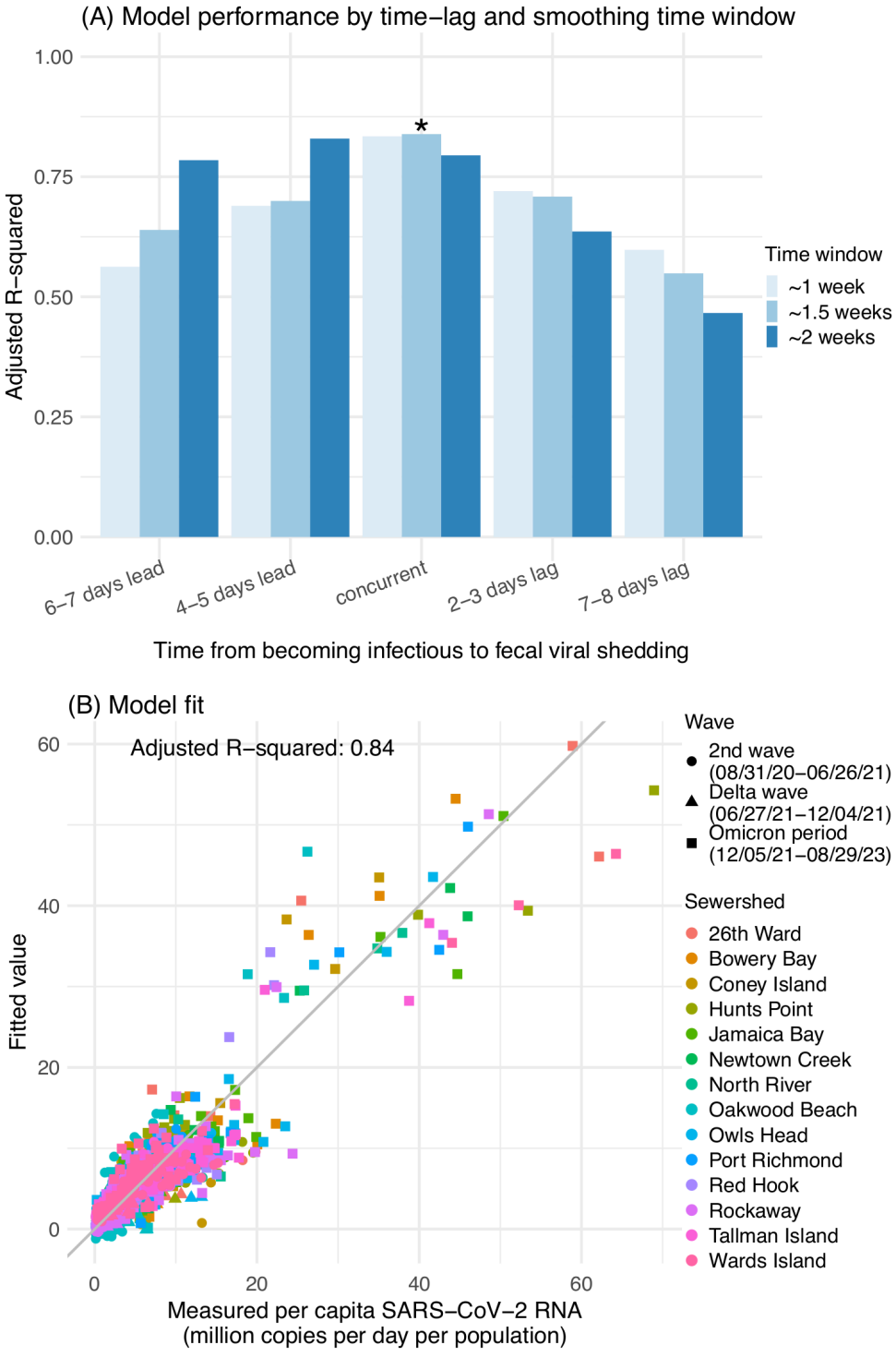

Fig 3. Identified time-periods with intensified transmission in any of 14 NYC sewersheds. (A) shows an example of the measured (dots) and expected wastewater SARS-CoV-2 viral load (blue line = median; darker blue area = 50% CI and lighter blue area = 95% CI), and identified anomalies with SARS-CoV-2 viral load exceeding the expected (red labels). (B) shows the distribution of all identified anomalies. Asterisks indicate time-periods that exceeded the expected wastewater SARS-CoV-2 viral load with a frequency higher than chance assuming random occurrence per a bootstrapping test (* for $P < 0.1$ and ** for $P < 0.05$). Spatial distribution of the anomalies is shown in Fig S4.

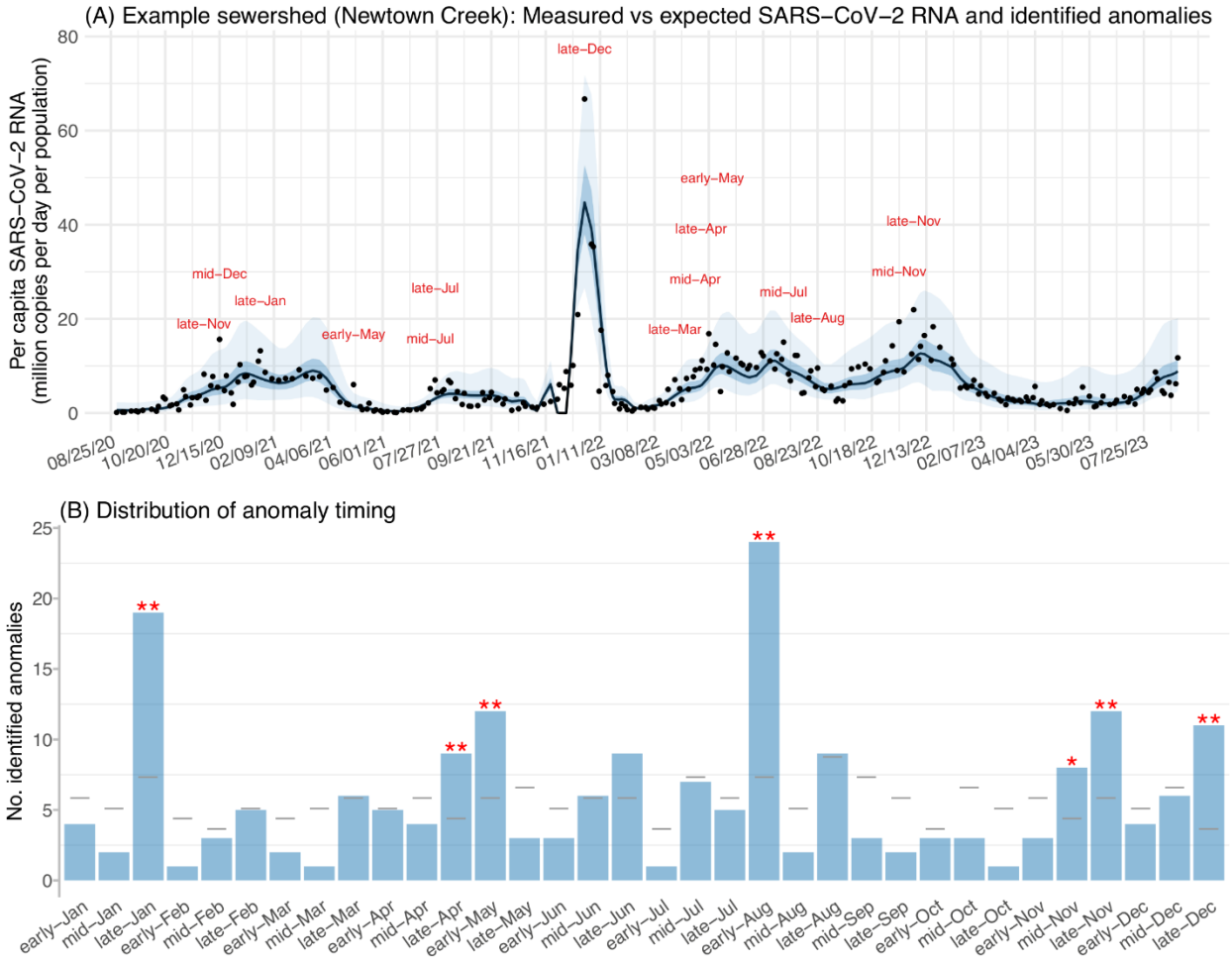

Supplement Tables and Figures

Table S1. Summary statistics for the wastewater samples

statistics	value	n	percentage
Total No. of samples	-	3794	100%
Day of sampling	Sunday	1834	48.3%
Day of sampling	Tuesday	1736	45.8%
Day of sampling	Wednesday	126	3.3%
Day of sampling	Monday	98	2.6%
Sampling frequency	2 per week	1610	73.7%
Sampling frequency	1 per week	574	26.3%
Calendar time	late-Aug	168	4.4%
Calendar time	early-Aug	140	3.7%
Calendar time	late-Jan	140	3.7%
Calendar time	mid-Jul	140	3.7%
Calendar time	mid-Sep	140	3.7%
Calendar time	late-May	126	3.3%
Calendar time	mid-Dec	126	3.3%
Calendar time	mid-Oct	126	3.3%
Calendar time	early-Jan	112	3%
Calendar time	early-May	112	3%
Calendar time	early-Nov	112	3%
Calendar time	late-Jul	112	3%
Calendar time	late-Jun	112	3%
Calendar time	late-Mar	112	3%
Calendar time	late-Nov	112	3%
Calendar time	late-Sep	112	3%
Calendar time	mid-Apr	112	3%
Calendar time	mid-Jun	112	3%
Calendar time	early-Apr	98	2.6%
Calendar time	early-Dec	98	2.6%
Calendar time	early-Jun	98	2.6%
Calendar time	late-Feb	98	2.6%
Calendar time	late-Oct	98	2.6%
Calendar time	mid-Aug	98	2.6%
Calendar time	mid-Jan	98	2.6%
Calendar time	mid-Mar	98	2.6%
Calendar time	mid-May	98	2.6%
Calendar time	early-Feb	84	2.2%
Calendar time	early-Mar	84	2.2%
Calendar time	late-Apr	84	2.2%
Calendar time	mid-Nov	84	2.2%
Calendar time	early-Jul	70	1.8%
Calendar time	early-Oct	70	1.8%

Calendar time	early-Sep	70	1.8%
Calendar time	late-Dec	70	1.8%
Calendar time	mid-Feb	70	1.8%

Table S2. Likelihood of having the same or higher frequency of anomalies during each calendar time as the observed, based on bootstrapping.

timing	number anomalies during this time	total number of anomalies	observed frequency	P-value: probability based on bootstrapping
early-Aug	24	198	0.1212	0.0000
late-Jan	19	198	0.0960	0.0002
late-Dec	11	198	0.0556	0.0008
late-Nov	12	198	0.0606	0.0124
early-May	12	198	0.0606	0.0138
late-Apr	9	198	0.0455	0.0286
mid-Nov	8	198	0.0404	0.0680
late-Jun	9	198	0.0455	0.1292
late-Aug	9	198	0.0455	0.5122
mid-Jun	6	198	0.0303	0.5364
late-Mar	6	198	0.0303	0.5380
late-Feb	5	198	0.0253	0.5850
early-Apr	5	198	0.0253	0.5860
mid-Jul	7	198	0.0354	0.6134
mid-Dec	6	198	0.0303	0.6546
late-Jul	5	198	0.0253	0.7060
mid-Feb	3	198	0.0152	0.7068
early-Oct	3	198	0.0152	0.7148
early-Dec	4	198	0.0202	0.7582
early-Jan	4	198	0.0202	0.8450
mid-Apr	4	198	0.0202	0.8490
early-Jun	3	198	0.0152	0.8900
early-Nov	3	198	0.0152	0.9384
early-Mar	2	198	0.0101	0.9386
late-May	3	198	0.0152	0.9634
mid-Oct	3	198	0.0152	0.9634
mid-Jan	2	198	0.0101	0.9686
mid-Aug	2	198	0.0101	0.9720
early-Jul	1	198	0.0051	0.9772
mid-Sep	3	198	0.0152	0.9788
late-Sep	2	198	0.0101	0.9830
early-Feb	1	198	0.0051	0.9888
late-Oct	1	198	0.0051	0.9924
mid-Mar	1	198	0.0051	0.9956

Table S3. Estimated patterns of SARS-CoV-2 fecal viral shedding in wastewater, using RT-qPCR data alone through April 11, 2023. All estimates here are based on RT-qPCR measures.

model	wave	shedding rate (billion copies per day per infectious person, mean and 95% confidence interval)	lag (days)	number of samples	adjusted R^2
Include all variant waves	2nd wave (08/31/20-06/26/21)	1.45 (1.36, 1.54)	0	3	0.84
	Delta wave (06/27/21-12/04/21)	1.16 (0.88, 1.44)	0	3	0.84
	Omicron period (12/05/21-04/11/23)	0.59 (0.58, 0.6)	0	3	0.84
Stratified by wave/ period	2nd wave (08/31/20-06/26/21)	1.44 (1.37, 1.52)	0	4	0.74
	Delta wave (06/27/21-12/04/21)	1.09 (0.91, 1.27)	-5	4	0.37
	Omicron period (12/05/21-04/11/23)	0.59 (0.58, 0.61)	0	3	0.86
	Omicron BA.1 (12/05/21-03/05/22)	0.59 (0.56, 0.61)	0	3	0.91
	After BA.1 (03/06/22-04/11/23)	0.72 (0.69, 0.75)	-5	4	0.76

Fig S1. Per-capita wastewater SARS-CoV-2 viral load in each of the 14 NYC sewersheds during the 2nd wave. Dots showed aggregated wastewater SARS-CoV-2 viral load for each week. For comparison, we overlay the corresponding estimates of infection prevalence (blue line = median; darker blue area = 50% CI and lighter blue area = 95% CI). The sewersheds are ordered by the mean viral load during this time period (from the highest to the lowest).

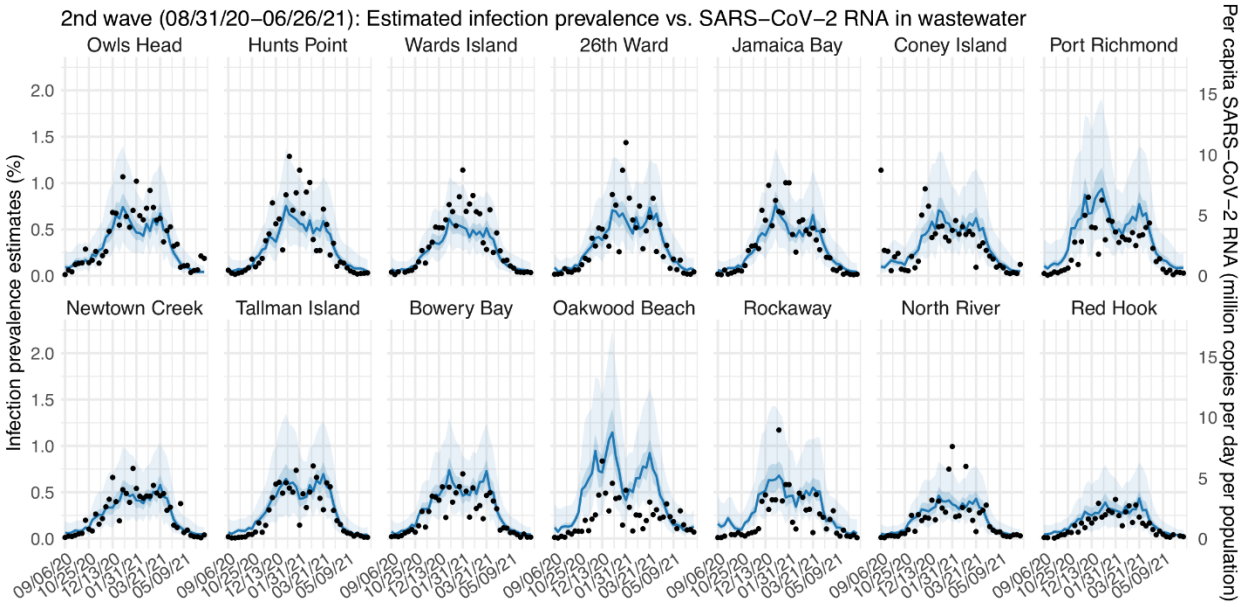

Fig S2. Per-capita wastewater SARS-CoV-2 viral load in each of the 14 NYC sewersheds during the Delta wave. Dots showed aggregated wastewater SARS-CoV-2 viral load for each week. For comparison, we overlay the corresponding estimates of infection prevalence (blue line = median; darker blue area = 50% CI and lighter blue area = 95% CI). The sewersheds are ordered by the mean viral load during this time period (from the highest to the lowest).

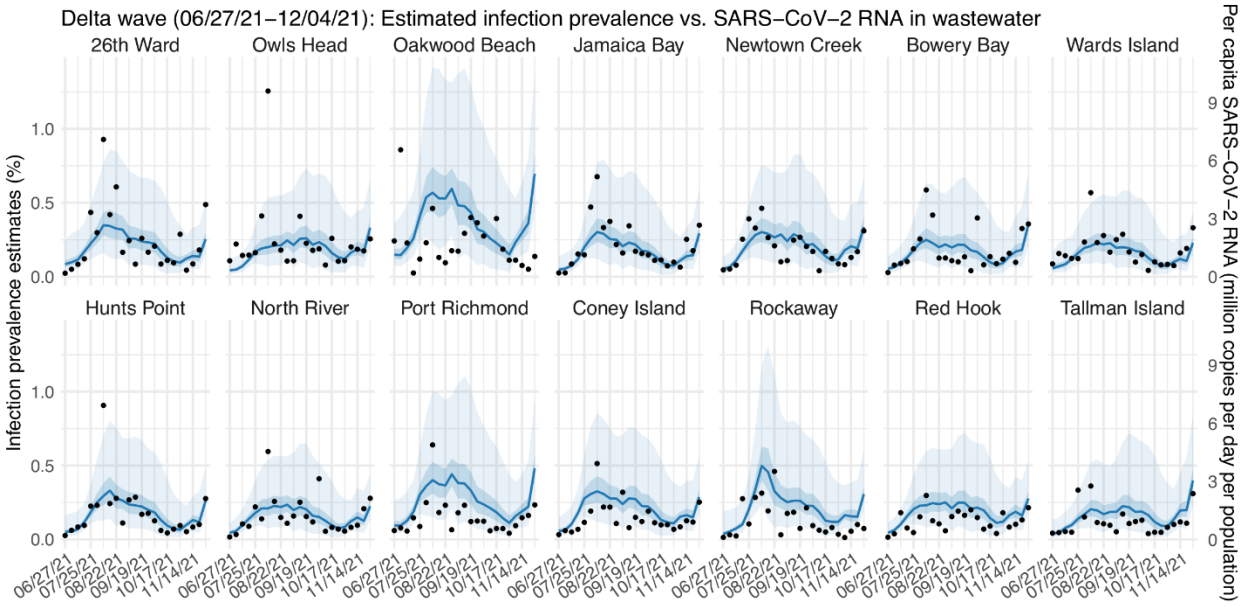

Fig S3. Per-capita wastewater SARS-CoV-2 viral load in each of the 14 NYC sewersheds during the Omicron period. Dots showed aggregated wastewater SARS-CoV-2 viral load for each week. For comparison, we overlay the corresponding estimates of infection prevalence (blue line = median; darker blue area = 50% CI and lighter blue area = 95% CI). The sewersheds are ordered by the mean viral load during this time period (from the highest to the lowest).

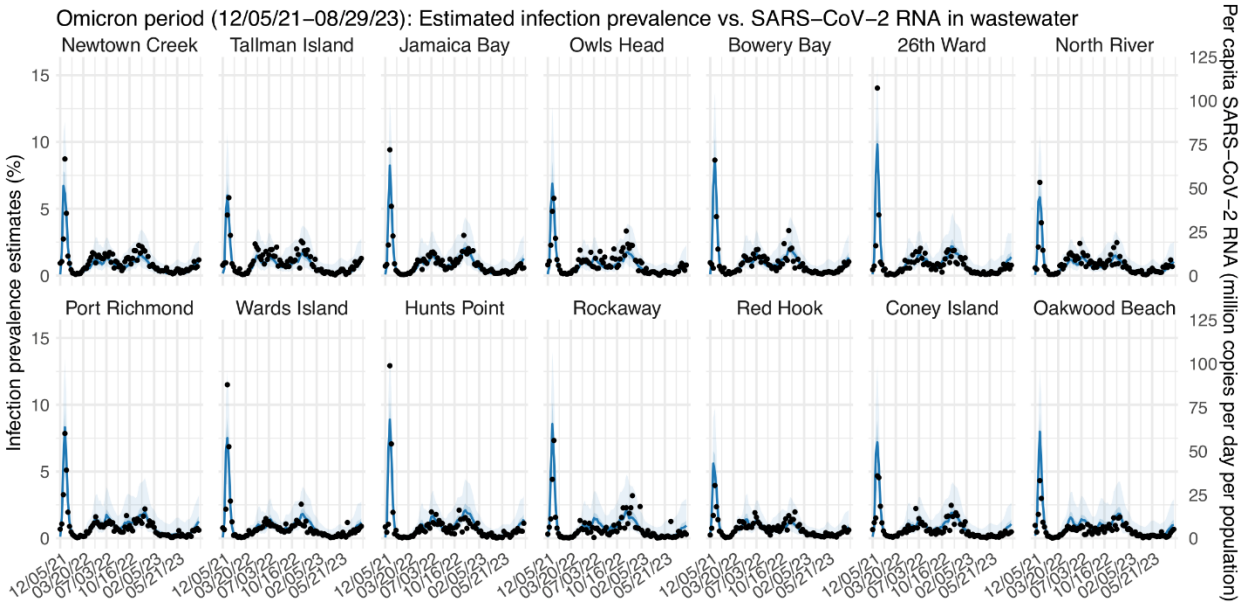

Fig S4. The total number of anomalies identified for each sewershed during the study period (n; see numbers in the map; darker colors indicate larger numbers).